Eur Biophys J (2000) 28: 674–682

ARTICLE

Hyeon S. Son · Mark S.P. Sansom

Simulation studies on bacteriorhodopsin α-helices

Received: 5 July 1999 / Revised version: 5 October 1999 / Accepted: 15 October 1999

Abstract Bacteriorhodopsin (BR) is a membrane protein which pumps protons through the plasma membrane. Transmembrane BR helical segments are subjected to simulation studies in order to investigate the effect of bilayer environment in various simulation conditions. A bilayer potential is introduced to the system to mimic the lipid membrane. The structures from the simulations are compared with the experimentally determined structures in terms of geometrical properties. Electrostatic contribution to the helix packing is also investigated. The simulation results show that the packing geometry of the transmembrane helices is highly affected by the bilayer potential. The results obtained from the simulations may be used for further simulation studies and analysis in investigating transmembrane helix packing.

Key words Bacteriorhodopsin · Simulated annealing · Molecular dynamics simulation · Bilayer potential

Introduction

Halobacterium halobium synthesizes a particular region of the membrane that converts energy from visual light into stored energy by pumping protons through the plasma membrane. This region is the purple membrane, of which bacteriorhodopsin (BR) is the major protein. This protein has a prosthetic group, retinal, which is responsible for the proton pump (Stoeckenius and Rawen 1967; Oesterhelt and Stoecknius 1973). BR forms an extremely regular two-dimensional array (Blaurock and Stoeckenius 1971). The seven-transmembrane domain structure of BR was first determined at 7.0 Å resolution by electron microscopy (Henderson and Unwin 1975). This structure has been extended to near atomic resolution, 3.0 Å (horizontal) and 10.0 Å (vertical), providing invaluable information about transmembrane helix packing (Henderson et al. 1990). The vertical resolution of the structure has been improved to 4.3 Å (Grigorieff et al. 1996). BR has seven transmembrane helices (TMHs), which are roughly perpendicular to the plane of the lipid bilayer, and the helices are linked by the extracellular and the cytoplasmic loops. Helices A to G are arranged in anticlockwise order when they are viewed from outside the bilayer. All neighbouring helices are anti-parallel except for the GA pair which is formed by the first helix (A) and the last helix (G) which close the bundle. Helices B, C and F contain proline residues that are believed to induce the helix kinks (Barlow and Thornton 1988; Sankararamakrishnan and Vishveshwara 1992). The kink angles calculated from the experimentally determined BR structure are shown in Table 1 along with other geometrical values (Fig. 1 shows the definitions of helix orientation).

Simulated annealing via molecular dynamics (SA/MD, Kirkpatrick et al. 1983) has been used successfully to refine structures from X-ray diffraction and from NMR spectroscopy (Brünger et al. 1990; Karplus and Pesko 1990; Brünger 1992). Similar SA/MD methods may be able to predict structures provided that the initial structure prior to the simulation is reasonably close to the native conformation. To set the initial structure, information from experiments and theoretical studies could be used. For example, membrane-spanning regions could be predicted and the alignment of the transmembrane segments could be determined by labelling experiments (Hubbell and

H.S. Son (✉)[1] · M.S.P. Sansom
Laboratory of Molecular Biophysics,
The Rex Richards Building,
Department of Biochemistry, University of Oxford,
South Parks Road, Oxford OX1 3QU, UK

Present address:
[1] National Creative Research Initiative Center
for Superfunctional Materials,
Department of Chemistry,
Pohang University of Science and Technology,
San 31, Hyojadong, Namgu, Pohang 790-784, Korea
e-mail: hyeon@chem.postech.ac.kr

Table 1 Geometrical analysis of bacteriorhodopsin (BR) transmembrane helices (energy minimized data: Henderson et al. 1990)
(a) Kink angles (θ_k), tilt angles (ζ), rotation angles (η) and helix lengths (l_h)

BR helix	A	B	C	D	E	F	G
θ_k (°)	–	5.8	17.2	–	–	22.0	–
ζ (°)	21.1	174.3	8.3	170.7	14.7	164.0	15.6
η (°)	241.0	327.9	79.6	0.7	333.4	112.2	259.7
l_h (Å)	31.29	36.5	34.4	32.4	34.1	37.5	34.5

(b) Crossing angles (Ω) and the closest distances (d_c)

BR dimer	AB	AC	AD	AE	AF	AG	BC	BD	BE	BF	BG
Ω (°)	−157.9	28.7	−161.7	26.0	−163.4	8.0	−172.1	−5.5	−159.6	21.8	−161.5
d_c (Å)	8.1	14.2	21.8	27.9	19.6	9.5	8.8	18.4	21.1	15.3	9.8
BR dimer	CD	CE	CF	CG	DE	DF	DG	EF	EG	FG	–
Ω (°)	166.6	18.6	−155.9	23.6	−156.6	22.1	−163.5	−168.8	18.1	−170.9	–
d_c (Å)	9.5	11.4	11.0	11.6	8.5	12.1	16.2	10.7	19.1	8.1	–

Altenbach 1994). Herzyk and Hubbard (1995, 1998) derived restraints from such information to produce models of transmembrane domains. The proposed "two-stage folding" model proposed by Popot and Engelman (1990) suggests that the process of folding for transmembrane proteins can be divided into two distinctive thermodynamic stages: firstly, stable helices are formed; and secondly, these TMHs pack together to form the native structure of the integral membrane protein. BR has proven an excellent testing system to verify this hypothesis. A number of experiments on isolated BR segments have been carried out and it has been successfully shown that reconstituting BR (in vitro) is possible (Arseniev et al. 1988; Barsukov et al. 1992; Kahn and Engelman 1992; Pervushin and Arseniev 1992; Orekhov et al. 1994).

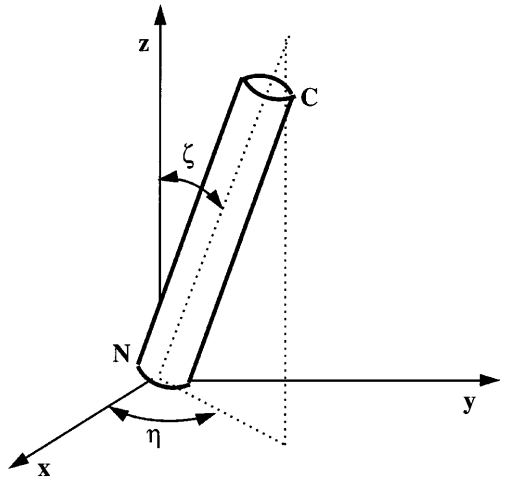

Fig. 1 Definition of tilt (ζ) and rotation (η) angles. The *xy* plane represents the lipid bilayer plane and the *z*-axis represents the bilayer normal. A transmembrane helical segment is drawn simplified as a cylinder. The rotation angle is a measure of in which direction a helix is inclined and the tilt angle is a measure of how much is the inclination

The lipid bilayer environment plays a crucial role in TMH packing. Attempts have been made to simulate the behaviour of membrane protein segments with the lipid environment (Edholm and Jähnig 1988; Jähnig and Edholm 1992; Milik and Skolnick 1993, 1995). MD studies of BR helices in an explicit dimyristoylphosphatidylcholine bilayer by Woolf (1997, 1998) were significant improvements in treating the membrane environment. Membrane lipids are amphipathic molecules and so a bilayer has two hydrophilic surfaces with a hydrophobic region in between. An exponential type of function suggested by Edholm and Jähnig was employed in our study to represent the hydrophobic potential differences experienced by constituent amino acids of the helices. BR monomers and dimers have been simulated with the bilayer potential and the results are discussed in later sections.

Materials and methods

BR sequence

Only the seven transmembrane helical segments are simulated. The residues are labelled such that the residue numbers restart from the first residue of each segment:

Helix A: E_1WIWL_5ALGTA$_{10}$LMGLG$_{15}$TLYFL$_{20}$VK-GM
Helix B: P_1DAKK$_5$FYAIT$_{10}$TLVPA$_{15}$IAFTM$_{20}$YLS-ML$_{25}$L
Helix C: Y_1WARY$_5$AD-WLF$_{10}$TTPLL$_{15}$LLDLA$_{20}$LLV
Helix D: T_1ILAL$_5$VGADG$_{10}$IMIGT$_{15}$GLVGA$_{20}$L
Helix E: F_1VWWA$_5$ISTAA$_{10}$MLYIL$_{15}$YVLFF$_{20}$GFT
Helix F: E_1VAST$_5$FKVLR$_{10}$NVTVV$_{15}$LWSAY$_{20}$PVV-WL$_{25}$IGS
Helix G: N_1IETL$_5$LFMVL$_{10}$DVSAK$_{15}$VGFGL$_{20}$ILL-RS$_{25}$RA

SA/MD studies

The SA/MD protocol has been used to generate ensembles of BR helices (monomers and dimers). The SA/MD method used is similar to that described by Nilges and Brünger (1991) for predicting the structure of GCN4 helix dimers, a prediction which was subsequently shown to be in agreement with experimental structural data. This method generates ensembles of structures so that statistical analyses over the variation of structures are possible. For each helix (A–G), only Cα atoms were used to build an ideal helix structure (3.6 residues per turn and a rise per residue of 1.5 Å along the helix axis). The remaining atoms were superimposed on the corresponding Cα atoms. For dimer simulations, the initial dimers were set to have similar orientations to energy minimized (EM)-determined BR dimers. Thus helices were rotated about their axes to make two specific residues (one from each helix) to face to each other: A (Met12) and B (Ala15), B (Val13) and C (Thr11), C (Tyr5) and D (Ile13), D (Ala8) and E (Ala10), E (Leu15) and F (Alg10), F (Ala19) and G (Phe7) and G (Val16) and A (Gly15). These backbone and sidechain atoms were then released to be "grown out" from the fixed Cα atoms. Annealing started at 1000 K, during which geometrical interactions and later a repulsive van der Waals term were slowly introduced. The system was then cooled down slowly to 300 K, keeping the Cα atoms fixed at their original locations. Ten structures (monomers) and five structures (dimers) from this stage were then fed into the MD stage (this is a MD stage as a module of the SA/MD protocol) to generate ensembles of 50 and 25 structures (50 structures in monomer simulation and 25 in dimer simulation). In this stage the Cα atoms were gradually allowed to move from their initial locations. A temperature of 500 K was assigned to the system. An electrostatic term was introduced by scaling polar sidechain partial atomic charges as the temperature was reduced from 500 K to 300 K. Three alternative treatments of sidechain partial charges were employed: (1) all set to zero; (2) gradually scaled to 50% of their standard values (i.e., as in the CHARMm parameter set); (3) gradually scaled to 100% of their standard values. For the treatment of nonbonded interactions, a distance-dependent dielectric was employed ($\varepsilon = r$, where r is the interatomic distance, or $\varepsilon = 2.0$ accordingly). On reaching 300 K, a 5 ps burst of constant temperature dynamics was performed, followed by 1000 steps of conjugate gradient energy minimization. These ensembles were then subjected to the analysis. Xplor V3.0 (Brünger 1992) and CHARMm V23 were used with the CHARMm PARAM19 (Brooks et al. 1983) parameter set to perform the simulations throughout.

MD studies with bilayer potential

A U-shaped potential form is used to represent the lipid bilayer environment. The residue-based bilayer potential (V_b) is defined as follows:

$$V_b = \begin{cases} \frac{1}{2}\sum_i^N h_i e^{-(|z_i|-d)/\lambda} & \text{for } |z_i| \geq d \\ \frac{1}{2}\sum_i^N h_i (2 - e^{(|z_i|-d)/\lambda}) & \text{for } |z_i| < d \end{cases}$$

where z_i is the coordinate of the residue concerned, $2d$ is the thickness of the bilayer, h_i is the hydrophobicity of the residue concerned, and where the summation is over the N residues of a helix. λ is a coefficient governing the shape of the curve in the region corresponding to the transition between hydrophilic and hydrophobic environments $\lambda = 2.0$ Å is used to provide a smooth transition. This potential form is also described in detail in our previous report (Son and Sansom 1999). A hydrophobicity scale developed by Engelman et al. (GES scale, 1986) was used to mimic the lipid bilayer environment.

MD simulations were performed for the seven BR monomers (A–G), and seven adjacent helix pairs (AB, BC, CD, DE, EF, FG, GA). Initial structures were selected from the SA/MD simulation described in the previous section. The geometrical average structure was found using a simple arithmetic calculation over the ensemble of structures generated by the SA/MD simulation. Root mean square deviation (RMSD) values were calculated between the individual simulated ensemble structures and the average structure. The structure which had the least RMSD value was chosen to be the initial model to be used in the MD simulation. One thousand cycles of adopted basis Newton Raphson (ABNR) energy minimization were performed on the initial model. The temperature was gradually increased from 0 to 300 K in steps of 50 K during the heating state. At each temperature, 0.5 ps of MD simulation was allowed. Rescaled velocities were assigned to the system every 0.1 ps during heating, and every 1 ps during the equilibrium period of 22 ps. Having equilibrated the system, 250 ps of further simulation was performed, while the system temperature was kept at 300 K by coupling to a temperature bath (Berendsen et al. 1984). The time step was 0.001 ps. A total of 3000 MD simulated structures were saved for further conformational analysis. The bilayer potential described in the previous section was implemented using the MMFP module of CHARMm. Hydrophobicity scale values were assigned to the constituent residues in order to reflect the bilayer potential environment. The N-terminus of the helix was assigned $h_i = 10$ kcal/mol, and $h_i = 20$ kcal/mol was assigned to the C-terminus to take into account the potential energy difference of bringing unsatisfied H-bonding N···H and C═O groups from an aqueous environment to the hydrophobic bilayer environment.

Results

SA/MD simulation

The kink angles of the simulated BR monomers are shown in Table 2. Three different electrostatic condi-

Table 2 Results of BR SA/MD simulations: (a) The kink angles (θ_k) from the BR structures determined by various methods (EM data: Henderson et al. 1990; NMR data: Barsukov et al. 1992); (b) the kink angles; (c) the crossing angles (Ω); (d) the closest distances (d_c). In the SA/MD simulation, different electrostatic conditions are considered for polar sidechain partial charges: (1) no partial charges, (2) charges scaled to 50% of their standard values, (3) 100% of values, i.e. no scaling (with distant-dependent dielectric of $\varepsilon = r$, where r is the interatomic distance), (4) 100% of values (with constant dielectric of $\varepsilon = 2.0$)

BR helix	Helix B		Helix C		Helix F		
(a) Kink angle (SD) (°)							
BR structure of EM	5.8		17.2		22.0		
BR structure of NMR	27		–		25		
SA/MD condition (1)	23(11)		37(12)		76(11)		
SA/MD condition (2)	22(9)		36(14)		75(11)		
SA/MD condition (3)	24(9)		55(17)		73(11)		
SA/MD condition (4)	27(9)		40(16)		66(15)		
	in AB	in BC	in BC	in CD	in EF	in FG	
(b) Kink angle (SD) (°)							
SA/MD condition (3)	21(10)	34(17)	36(17)	40(19)	53(13)	58(15)	
SA/MD condition (4)	24(11)	22(11)	19(8)	42(14)	30(12)	53(11)	
BR dimer	AB	BC	CD	DE	EF	FG	GA
(c) Crossing angle (SD) (°)							
SA/MD condition (3)	−170(13)	−163(7)	−170(20)	−170(15)	−171(15)	−168(7)	−0.2(12.5)
SA/MD condition (4)	−165(8)	−165(10)	−166(15)	−174(21)	−175(9)	−161(7)	14.75(7.9)
(d) Inter-helical closest distance (SD) (Å)							
SA/MD condition (3)	7.5(0.8)	8.2(0.9)	7.4(1.3)	8.7(0.9)	8.3(0.7)	8.5(0.9)	8.3(0.7)
SA/MD condition (4)	7.7(0.8)	8.3(0.6)	7.9(0.8)	7.5(1.2)	8.4(0.6)	8.6(0.8)	8.6(0.7)

tions were set for the simulations to investigate their possible effects on the helix kink. The kink angles from the simulated structures are larger than those from experimentally determined structures. The following observations can be summarized:

(1) In helix B, the kink angle is insensitive to the electrostatic conditions set up for the simulations. Even though the kink angle from the SA/MD simulation agrees with the NMR structure, it is far greater than that of EM-determined structures.
(2) In helix C, the kink angle from the simulation shows that the angle is sensitive to the electrostatic conditions and it is greater than in the EM case.
(3) In helix F, the kink angle is not sensitive to the electrostatic conditions, and the angle is far greater in the simulated structures than in experimentally determined structures.
(4) SA/MD simulated dimers show kinks less than those of monomer simulation.

The NMR experiments by Barsukov et al. (1992) were carried out on isolated segments. Thus the presence of other helices within a bundle could have affected the behaviour of the system, and the dimer simulation results agree with this assumption. The effect of electrostatic interaction is analyzed in terms of (ϕ, ψ) values for the residues around the proline residue for each monomer. The structures from the EM experiment show quite different values from those simulated, and no simulated structure agrees with the EM data. The (ϕ, ψ) values do not show many changes to different electrostatic conditions (except some changes observed in helix C). Thus the electrostatic force was not responsible for the helix kink except in helix C; in other words, the interactions of charged polar sidechains are not generally (at least directly) responsible for the helix kink in the SA/MD simulations carried out for BR. However, because BR helix C has the charged residues located around the proline residue, the electrostatic conditions do strongly affect the kink in helix C.

Helix crossing angles (Ω) were defined as suggested by Chothia et al. (1981). A crossing angle is a measure of how two helices mutually interact in a given packing environment. In particular, analysis of the crossing angles can be used to see if the "ridges into grooves" (Chothia et al. 1981) packing of helices is taking place. Table 2 shows the crossing angles from SA/MD simulated dimers: AB, BC, CD, DE, EF, FG and GA. Even though some results are within the range of standard deviation, they are not convincingly accurate to say that the SA/MD simulation method alone produced a reasonable model of BR dimers. Particularly, the dimer CD from EM has a positive crossing angle (166°), while the SA/MD simulation produced a negative one (−170°). However, according to the "ridges into grooves" theory, SA/MD produced a correct crossing angle. Table 2d shows the closest distance between all the simulated pairs. Initially the helix rods were set 9.4 Å apart; the closest distances calculated show that helices became even more compact during the simulation.

MD simulation

The proline-containing BR helices B, C and F were subjected to MD simulations. The bilayer potential was

set to have a thickness of 30 Å. Figure 2 shows the variation of kink angles along MD trajectories. Helix kink angles were stabilized after ~20 ps of a MD run. An abrupt switching of the angles was observed for the segments C and F. These abrupt changes are due to the introduction of the bilayer potential (the initial structures were taken from SA/MD simulations in which the bilayer environment was not included). Smaller (than SA/MD produced) kink angles were produced after stabilization because the helices were stretched owing to the hydrophilic terms set to the termini of the segments. The average kink angles are B 7.3(3.8)°, C 14.3(5.4)° and F 29.3(8.7)°. These values agree better with the values from the experimentally determined structure. This suggests that the bilayer potential is responsible for the smaller helix kinks in prolin-containing BR helices, i.e., the existence of the lipid bilayer influences the transmembrane helical conformation. The same helices were

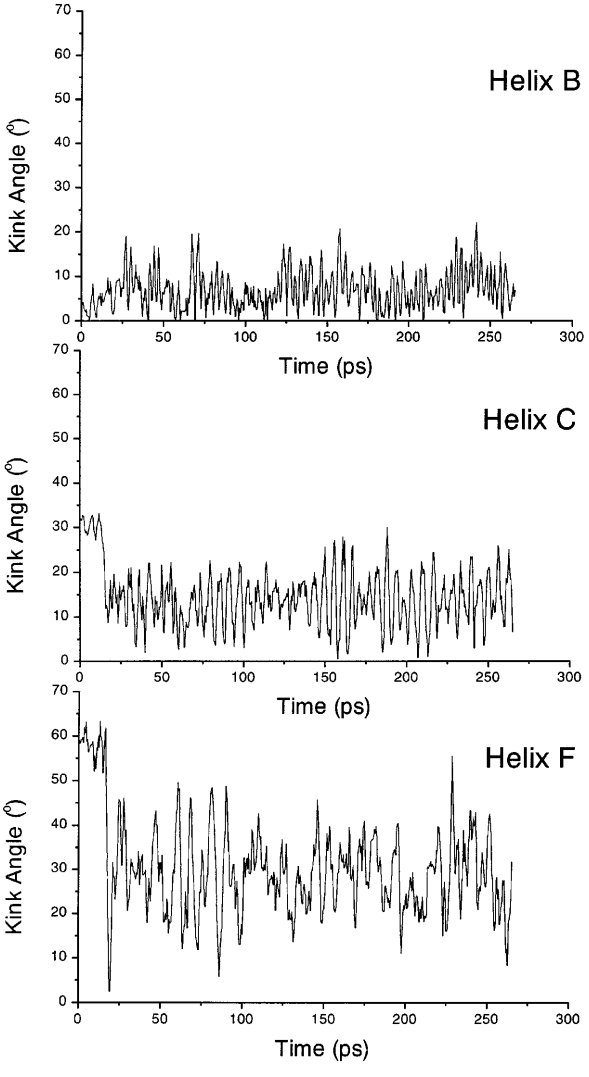

Fig. 2 The variation of kink angles during molecular dynamics (MD) monomer simulation. Helices B, C and F are set in the lipid environment. The labels on the *x*-axis are scaled such that the simulation times from 0 ps to 265 ps are shown

(MD) simulated with a different bilayer thickness (20 Å). The kink angles found from the new simulations are B 9.8(4.9)°, C 9.4(4.9)° and F 32.5(8.7)°. The thin bilayer potential increased the kink angle in the segments B and C, but decreased the angle in the segment F. Therefore the relative thickness of the bilayer with respect to the length of the helical segment affects the degree of kinking.

The tilt angle and the rotation angle (as defined in Fig. 1), along with others, should be able to tell us how much the lipid bilayer affects helix orientation. Helices B, F and G show significant stability at the early stage of the MD simulation in terms of tilt angle. These helices all have longer helix lengths than the others. These long helices maintain orientational stability easily in the lipid environment. Considering the bilayer thickness and the potential implemented, it is a predictable result. It is energetically costly for the long helices (helices whose lengths are longer than the bilayer thickness) to have tilt angles greater than a certain angle which is determined by factors such as helix length and bilayer thickness. Long helices tend to have their termini outside the bilayer unless large kinks shorten the helix lengths, and because the termini are highly hydrophilic it is difficult for them to be buried inside the bilayer. Therefore the bilayer transition region acts as a high energy barrier to prevent the termini from being buried in the bilayer. Short helices (helices whose lengths are shorter than the bilayer thickness) have to be buried in the bilayer; either the N-terminus or C-terminus but not both termini can be outside the bilayer region at the same instance. One terminus acted as an anchor to fix a helix to the hydrophilic region of the bilayer while the other terminus was left buried inside the bilayer region. The buried terminus, though hydrophilic, did not experience high local energy barriers; hence it has a freedom to float within the bilayer region. The short helix D showed an increase in tilt angle as the simulation progresses. The average value of the tilt angle for B, F and G are B 2.7(0.7)°, F 1.5° and G 2.2(2.2)°.

The average helix lengths calculated from the stabilized trajectories are A 33.3(0.5) Å, B 36.5(0.5) Å, C 31.5(0.7) Å, D 28.4(0.5) Å, E 31.8(0.4) Å, F 39.0(1.0) Å and G 37.5(0.5) Å. At the beginning of the simulation the initial structures had idealized helix lengths (1.5 Å rise per residue). The idealized helix lengths are A 34.5 Å, B 37.5 Å, C 33.0 Å, D 30.0 Å, E 33.0 Å, F 40.5 Å and G 39.0 Å. The segments used in this calculation contain terminal patches; therefore these values are expected to be longer than the values calculated from the experimentally determined structure. All the simulated helices show shorter helix lengths than the idealized ones. This is no surprise. All the simulated structures have some degree of bends or kinks to shorten the helix lengths. However, this helix length analysis reveals that the proline-containing helices C and F have shorter helix lengths in the region of 0–20 ps of trajectory. In this region, helix kinks are obviously large (Fig. 2). Therefore, for these helices, kinks around the proline residues

are the obvious reason for reducing the helix length, while for other helices the reduced helix lengths are due to the bends over all the constituent residues. Therefore, the helix length analysis together with the kink analysis would roughly determine whether a helix is bent or kinked. Another aspect of the helix length analysis is that it tells us whether the system is stabilized or not. For example, if the stability is determined for each observable, e.g., kink angle or tilt angle, then the overall stability could be overlooked. For this reason, all the average values calculated in this study are from the regions where helix lengths are stabilized. The rotation angle variation was observed during the simulation. All the helices continuously swiveled about the bilayer normal axis (*z*-axis). The bilayer potential mainly holds the two ends of the helices (N- and C-termini of the helices) to the surfaces of the lipid bilayer by maintaining the hydrophilic contacts with the helix termini. For "long helices", this was achieved by bending the helices or by tilting the segments. This tendency is in equilibrium with the hydrophobic forces represented by the hydrophobicity scale values. For the same reason, "short helices" do not show bends or kinks at any time throughout MD trajectories.

Proline-containing helix dimers AB, BC, CD, EF and FG were MD simulated. Helix C in dimer BC shows initial high kinks and in dimer CD it also shows a "switching" behaviour between low and high kinks along the trajectory (Fig. 3). It was observed that inter-helical hydrogen bonds between B (Thr10) and C (Asp44) in dimer BC and C (Thr12) and D (Asp32) in dimer CD were responsible for the high kinks. The hydrogen bonding pulls the helices together in such a way that the kink angle is increased and this pattern remained stable until an external force broke the bonds (the EM-determined structure shows that there are no inter-helical hydrogen bonds in dimers BC and CD). Average kink angles for stabilized MD steps are B (in AB) 19.5(3.8)°, B (in BC) 15.7(5.4)°, C (in BC) 10.3(7.1)°, C (in CD) 13.6(6.4)°, F (in EF) 20.7(5.3)° and F (in FG) 26.8(4.9)°. These values are not in agreement with the values obtained from the EM-determined BR structure. It was shown, in monomer MD simulation, that the kink angles were similar to the EM values. The only obvious difference between these two kinds of simulations is the number of helices in the system. Therefore it should be concluded that the existence of other helices could alter the orientation of segments significantly. Furthermore, simulations in different dimer pairs yield different kink angles. This means that sidechain interactions are different in different pairs, and so are the helix-helix interactions. The orientation of dimers should be different and therefore observed kink angles should be different from the ones observed in monomer simulations.

The average crossing angles (Ω) during the MD simulations are AB 176.2(2.5)°, BC 170.7(5.2)°, CD 169.3(4.5)°, DE 164.4(8.3)°, EF 167.1(4.2)°, FG 158.6(3.0)° and GA 13.0(2.6)°. The crossing angle trajectories show that helix-helix interaction is stabilized at the early stages of the simulations. The "ridges into grooves" theory (Chothia et al. 1981) predicts that all the crossing angles for the pair of anti-parallel helices should be negative. This prediction is satisfied except for the DE helix pair. Another simulation without the bilayer potential was done to investigate this unexpected result. The average crossing angle from the simulation without the bilayer potential is DE 164.8(6.3)°. The results showed that simulation with bilayer potential produced a positive crossing angle, while non-bilayer simulation produced a negative crossing angle, i.e., the bilayer changes the predominant helix packing mode. Figure 4 presents the snapshots of the MD trajectories with and without bilayer potential. In the simulation with the bilayer potential, two short helices did not change their relative orientation along the trajectory, except at the beginning of the simulation, while the simulation without the bilayer potential showed more orientational fluctuation. The bilayer potential acted on the system in such a way that the movement of helices is more restrained so that helix-helix interaction favours the positive crossing angle. This also could mean that amino acids interact not only with other amino acids but also with their environment, i.e., the lipid bilayer, to produce the overall conformation. It is also observed that simulation with a bilayer potential tends to stabilize the system at the early stage (Fig. 4). The average inter-helical closest distances calculated from the stabilized trajectories are AB 8.1(0.3) Å, BC 9.1(0.3) Å, CD 8.7(0.5) Å, DE 8.1(0.5) Å, EF 8.5(0.4) Å, FG 8.7(0.2) Å and GA 9.0(0.2) Å. These are in good agreement with the values from the EM structure (Table 1).

Discussion

The main aims of the study described in this paper are: (1) to see if the introduction of a simple bilayer potential into the simulation would significantly affect the helix orientation and packing, and (2) to see if structures from simulations agree with experimentally determined structure(s) in terms of structural parameters. BR monomers and dimers were first simulated using the SA/MD protocol. The SA/MD simulations produced an ensemble of structures in which each member represents one of many local minima. Obvious observable properties such as helical kink and helix-helix crossing angle were calculated to characterize the simulated structures. Three different sets of electrostatic values were assigned for the polar sidechains of proline-containing BR helices. The kink angles calculated did not agree with the values from the EME-determined structure. Electrostatic interaction is not convincingly responsible for the helix kink/bend in the SA/MD simulation. SA/MD simulated structures could efficiently be used as initial structures for further MD simulations since the SA/MD method generally explores a wider range of conforma-

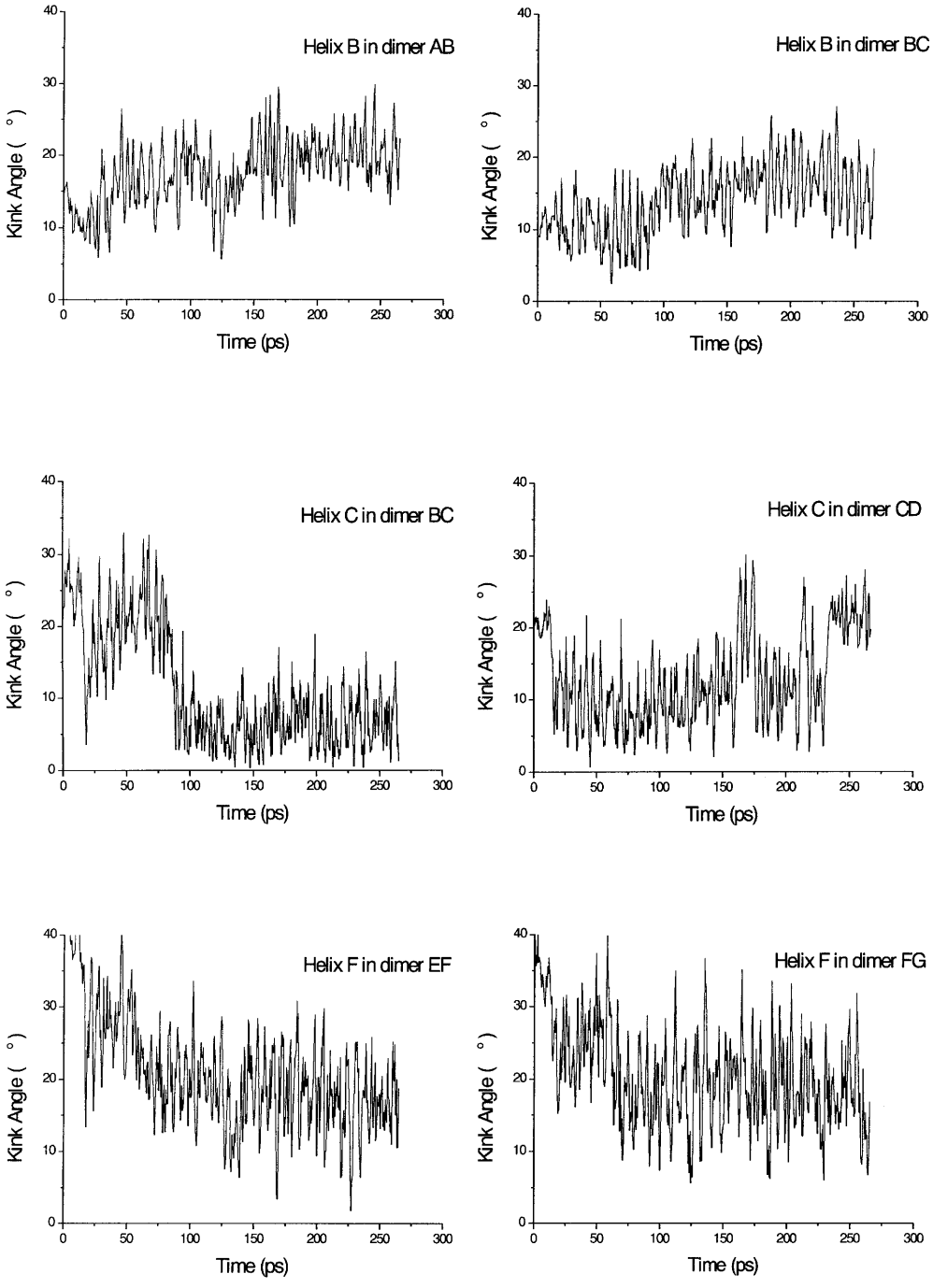

Fig. 3 The variation of kink angles during MD dimer simulation. The Pro-containing helix dimers AB, BC, CD, EF, FG and GA are MD simulated with the bilayer potential, and the variation of kink angles in the helices B, C and F are shown

tions (Sansom and Kerr 1995). In other words, the SA/MD simulation method can produce roughly defined structure(s) to be used as initial structure(s) to generate further refined structure(s) by the MD method. The structures with the least RMSD values from the average structures were chosen to be the initial structures of further MD simulation. Investigation of the bilayer effect is one of the objectives of this study. It is also possible to mimic the effect of the bilayer by the careful introduction of restraints to the system (Kerr et al. 1994; Sansom 1995). Intra- and inter-helical distances could be restrained to keep the helices within cutoff distances. These restraints are able to keep the helices inside the bilayer region. However, this method might not predict other possible effects of the bilayer. A more general representation of the bilayer environment was therefore needed. BR monomers and dimers were MD simulated with a simple bilayer potential. The monomer simulation results showed that kink angles now agreed with the values from the EM-determined structure. Therefore, the bilayer potential is one of the causes of helix kink. It was also shown that the length of a transmembrane helix is related to the kink angle. It is because both termini of a helix tend to be in contact with lipid surfaces (because

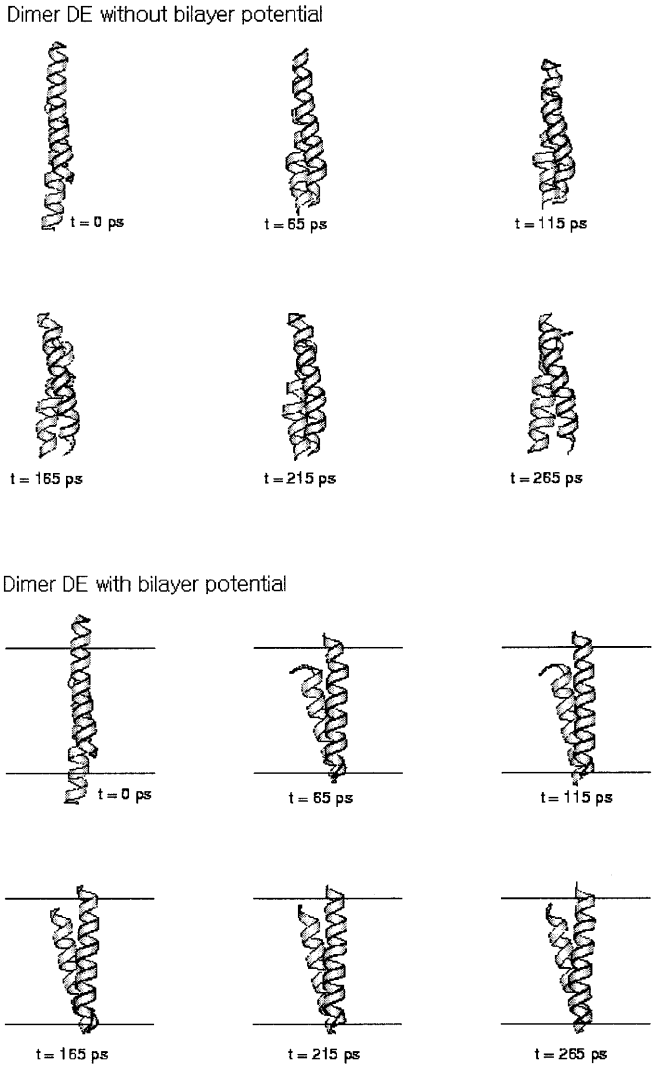

Fig. 4 The ribbon diagrams of the selected structures from MD trajectories of dimer (DE) simulation with and without bilayer potentials

they are hydrophilic). A long helix therefore shows a largest kink than a short helix. Here the proline residue acts as a hinge so that forces exerted on them cause the helix kinks around them. This is true for the current simulation system during which the bilayer thickness is kept constant. The situation would be more complicated in a real biological membrane system where the bilayer thickness varies significantly because of interaction between the lipids and the hydrophobic sidechains of transmembrane helical segments (Mouritsen and Bloom 1993). In the lipid-helix contact region, long TMHs induce a thick membrane. Considering this effect in a real system, the lipid bilayer thickness may be changed instead of the kink in a helix.

The effect of the bilayer was also investigated in terms of crossing angle. The crossing angle is the product of helix-helix and helix-bilayer interactions. The results of the simulation of dimer DE with and without the bilayer potential provide clear evidence that the bilayer potential mediates the helix packing. It also suggests that specific dimeric pairs could result in a different geometry in helix-helix packing. Analysis of closest distances showed that dimers were packed together effectively. Initially (at the beginning of SA/MD simulation), two residues in a dimer were set to point to each other according to the EM-determined BR dimer orientation. It is observed that these residues did not deviate much from their original locations, i.e., no helix has rotated about its own axis during the simulation. A MD simulation study of BR fragments was reported by Lakshmanan and Saraswathi (1996). It was suggested there that certain residues (charged ones and others) played a crucial role in the stability of the helices. The MD trajectory showed breaks of helicity owing to the charged residues and a high degree of fluctuation was reported during the simulation. This fluctuation was also observed in one of our dimer simulations (dimer DE without bilayer potential), and the absence of a bilayer potential was considered to be responsible in the previous discussion. In our simulation, charged residues did not affect the helix kink in the SA/MD stage. In the MD simulation stage, the bilayer potential prevented this break of helicity. It may not be simply that charged residues do not have any effect on the secondary structure; however, the simulation results presented here suggest that electrostatic interactions are not a major contributor in the presence of a lipid bilayer.

Conclusion

So far, we have concentrated on the effect of bilayer potential in the MD simulations. Our results suggest that the lipid bilayer environment strongly mediates the behaviour of the transmembrane helix orientation and packing. The continuum function (the bilayer potential function) is highly effective in describing the lipid membrane environment even though the form of the potential is extremely simple. The method and the data from the simulations may be useful for simulation studies in investigating transmembrane helix packing (Son and Sansom 1999).

Acknowledgements This work was supported by a grant from the Wellcome Trust. Our thanks to the Oxford Centre for Molecular Science for the use of computational facilities.

References

Arseniev AS, Maslennikov IV, Bytrov VF, Kozhich AT, Ivanov VT, Ovchinnikov YA (1988) Two-dimensional ^{1}H-NMR study of bacterioopsin-(34–65)-polypeptide conformation. FEBS Lett 231: 81–88

Barlow DJ, Thornton JM (1988) Helix geometry in proteins. J Mol Biol 201: 601–619

Barsukov L, Nolde DE, Lomiz AL, Arseniev AS (1992) Three-dimensional structure of proteolytic fragment 163–231 of bac-

terioopsin determined from nuclear magnetic resonance data in solution. Eur J Biochem 206: 665–672
Berendsen HJC, Postma JPM, Gunsteren WF van, Di Nola A, Haak JR (1984) Molecular dynamics with coupling to an external bath. J Chem Phys 81: 3684–3690
Blaurock AE, Stoeckenius W (1971) Structure of the purple membrane. Nature 233: 152–155
Brooks BR, Bruccoleri RE, Olafson BD, States DJ, Swaminathan S, Karplus M (1983) CHARMM: a program for macromolecular energy minimisation, and dynamics calculations. J Comput Chem 4: 187–217
Brünger AT (1992) X-PLOR version 3.0:system for X-ray crystallography and NMR. Yale University Press, New Haven
Brünger AT, Krukowski A, Erickson JW (1990) Slow-cooling protocols for crystallographic refinement by simulated annealing. Acta Crystallogr A46: 585–593
Chothia C, Levitt M, Richardson D (1981) Helix to helix packing in proteins. J Mol Biol 145: 215–250
Edholm O, Jähnig F (1988) The structure of a membrane-spanning polypeptide studied by molecular dynamics. Biophys Chem 30: 279–292
Engelman DM, Steitz TA, Goldman TA (1986) Identifying nonpolar transbilayer helices in amino acid sequences of membrane proteins. Annu Rev Biophys Chem 15: 321–353
Grigorieff N, Ceska TA, Downing KH, Baldwin JM, Henderson R (1996) Electron-crystallographic refinement of the structure of bacteriorhodopsin. J Mol Biol 259: 393–421
Henderson R, Unwin PNT (1975) Three-dimensional model of purple membrane obtained by electron microscopy. Nature 257: 28–32
Henderson R, Baldwin JM, Ceska TA, Zemlin F, Beckmann E, Downing KH (1990) Model for the structure of bacteriorhodopsin based on high-resolution electron cryo-microscopy. J Mol Biol 213: 899–929
Herzyk P, Hubbard RE (1995) Automated method for modeling seven-helix transmembrane receptors from experimental data. Biophys J 69: 2419–2442
Herzyk P, Hubbard RE (1998) Using the experimental information to produce a model of the transmembrane domain of the ion channel phospholamban. Biophys J 74: 1203–1214
Hubbell WL, Altenbach C (1994) Investigation of structure and dynamics in membrane proteins using side-directed spin labelling. Curr Opin Struct Biol 4: 566–573
Jähnig F, Edholm O (1992) Modelling of the structure of bacteriorhodopsin: a molecular dynamics study. J Mol Biol 226: 837–850
Kahn TW, Engelman DM (1992) Bacteriorhodopsin can be refolded from two independently stable transmembrane helices and the complementary five-helix fragment. Biochemistry 31: 6144–6151
Karplus M, Pesko GA (1990) Molecular dynamics simulations biology. Nature 347: 631–639
Kerr ID, Sankararamakrishnan R, Smart OS, Sansom MSP (1994) Parallel helix bundles and ion channels: molecular modeling via simulated annealing and restrained molecular dynamics. Biophys J 67: 1501–1515
Kirkpatrick S, Gelatt CD Jr, Vecchi MP (1983) Optimization by simulated annealing. Science 220: 671–680
Lakshmanan KL, Saraswathi V (1996) The stability of transmembrane helices: a molecular dynamics study on the isolated helices of bacteriorhodopsin. Biopolymers 38: 401–421
Milik M, Skolnick J (1993) Insertion of peptide chains into lipid membranes: an off-lattice Monte Carlo dynamics model. Proteins 15: 10–25
Milik M, Skolnick J (1995) A Monte Carlo model of fd and Pf1 coat proteins in lipid membranes. Biophys J 69: 1382–1386
Mouritsen OG, Bloom M (1993) Models of lipid-protein interactions in membranes. Annu Rev Biophys Biomol Struct 22: 145–147
Nilges M, Brünger AT (1991) Automated modelling of coiled coils: application to the GCN4 dimerization region. Protein Eng 4: 649–659
Oesterhelt D, Stoecknius W (1973) Functions of a new photoreceptor membrane. Proc Natl Acad Sci USA 70: 2853–2857
Orekhov VYu, Konstantine VP, Arseniev AS (1994) Backbone dynamics of (1–71) bacterioopsin studied by two-dimensional ^{1}H-^{15}N NMR spectroscopy. Eur J Biochem 219: 887–896
Pervushin KV, Arseniev AS (1992) Three-dimensional structure of (1–36) bacterioopsin in methanol-chloroform mixture and SDS micelles determined by 2D^{1}H-NMR spectroscopy. FEBS Lett 308: 190–196
Popot J-L, Engelman DM (1990) Membrane protein folding and oligomerization: the two-stage model. Biochemistry 29: 4031–4037
Sankararamakrishnan R, Vishveshwara S (1992) Geometry of proline-containing alpha-helices in proteins. Int J Pept Res 39: 356–363
Sansom MSP (1995) Twist to open. Curr Biol 5: 373–375
Sansom MSP, Kerr ID (1995) Principles of membrane protein structure. Biomembranes 1: 29–78
Son HS, Sansom MSP (1999) Simulation of the packing of transmembrane α-helix bundles. Eur Biophys J 28: 489–498
Stoekenius W, Rawen R (1967) A morphological study of *Halobacterium halobium* and its lysis in media of low salt concentration. J Cell Biol 34: 365–393
Woolf TB (1997) Molecular dynamics of individual α-helices of bacteriorhodopsin in dimyristolphosphatidylocholine. I. Structure and dynamics. Biophys J 73: 2376–2392
Woolf TB (1998) Molecular dynamics simulations of individuals α-helices of bacteriorhodopsin in dimyristoylphosphatidylocholine. II. Interaction energy analysis. Biophys J 74: 115–131